Jurnal Polimesin
Department of Mechanical Engineering
State Polytechnic of Lhokseumawe
http://e-jurnal.pnl.ac.id/polimesin
e-ISSN : 2549-1999 No. : 3 Month : June
p-ISSN : 1693-5462 Volume : 22 Year : 2024

Article Processing Dates: Received on 2024-02-27, Reviewed on 2024-05-15, Revised on 2024-05-26, Accepted on 2024-06-08 and Available online on 2024-06-29

A study on optimal parameter combinations for austempered ductile iron

Herry Oktadinata[1*], Dewin Purnama[2], Rizal Nurdian Hamzah[1], Agung Slamet Apriyan[1]
[1]Mechanical Engineering, Universitas Jenderal Achmad Yani, Cimahi, 40513, Indonesia
[2]Mechanical Engineering, Politeknik Negeri Jakarta, Depok 16425, Indonesia
*Corresponding author: herry.oktadinata@yahoo.com

Abstract

Nodular cast iron possesses a spherical graphite shape and exhibits mechanical properties closely resembling those of steel after heat treatment. The austempering method provides a means of enhancing the mechanical properties of nodular cast iron. This study aimed to investigate the optimal parameter combinations for Austempered Ductile Iron (ADI). The experiments involved varying the austenitization temperature and austempering time. Multiple tests were conducted to analyze the effects of austenitization temperature and tempering time on the microstructure, hardness, and impact toughness. The experimental samples were obtained from Y-block nodular cast iron austenitized at 850, 900, and 950°C for 90 min in an electric furnace. Subsequently, they were quenched in a salt bath at a temperature of 350°C and held for 60, 90, and 120 minutes before being cooled to room temperature. Mechanical tests and microstructure observations were performed on both the as-cast sample and after austempering. The microstructure was observed using an optical microscope before and after the etching. The research findings indicated that austempering increases the hardness and impact toughness of nodular cast iron. The highest hardness (46.8 HRC) was achieved from a parameter combination of an austenitization temperature of 850°C and an austempering time of 90 minutes. This particular sample also exhibited a relatively higher impact energy (3.8 J) compared to the others. The results of this study suggest that the austenitization temperature and tempering time exert an influence on the mechanical properties.

Keywords:
Austenitizing temperature, tempering time, hardness, impact toughness, microstructure.

1 Introduction

Nodular cast iron is used in many components that require superior mechanical properties compared to conventional cast iron. The typical microstructure of cast iron is composed of graphite nodules that are distributed in the metal matrix. Nodular cast iron has better strength and ductility compared to gray cast iron [1], [2].

The mechanical properties of as-cast nodular cast iron can be improved through an austempering heat-treatment process. Nodular cast iron that has undergone austempering heat treatment is called Austempered Ductile Iron (ADI) [1], [3], [4]. The ADI microstructure has a unique characteristic, namely spherical graphite in an ausferitic matrix. ADI's superior mechanical properties are mainly due to its ausferritic structure, consisting of acicular ferrite and high-carbon austenite [5]–[10].

ADI with excellent mechanical properties can be considered a replacement for conventional cast steel, forged steel, and even aluminum in many applications [3], [5], [11]. The excellent wear resistance of the ADI extends its life and provides adequate performance for a number of components, such as engine valves and cam shafts, which are often exposed to surface contact and external pressure, such as engine valves and cam shafts [5]. The cam shaft microstructure in the as-cast condition contained graphite nodules and a ferritic-pearlitic matrix structure, whereas the austemper cam shaft microstructure contained an ausferrite microstructure. Austemper cam shafts have a tensile strength that is 45%-50% higher than cam shafts in as-cast condition. The maximum tensile strength was obtained from the cam shaft austenitized at 900°C for 90 min [12].

The selection of the austemper parameters influences the mechanical properties and microstructure of the ADI formed [1], [4], [5], [13]–[15]. There are several important parameters in the austempering process, such as austenitization temperature, austenitization time, tempering temperature, and tempering time. The austenitization temperature had a significant effect on the formation of a homogeneous structure and the resulting mechanical properties. The homogeneity of the ADI microstructure metal matrix is highly dependent on the austenitization temperature and initial microstructure of nodular cast iron [16]. The austenitization temperature had a significant influence on the transformation rate during the subsequent austempering process. Increasing the austenitization temperature reduces the transformation rate during the austempering process. A higher austenitization temperature increases the austenite fraction and reduces the number of ferrite plates, and the ferrite plates become thicker and longer [16].

Austenite was more stable at lower austenitization temperatures. The growth rates of ferrite and austenite cells are greater at higher austenitization temperatures owing to the increase in austenite grain size. At higher temperatures, some carbides dissolve. The area fraction of carbides decreased at higher austenitization temperatures. Therefore, the hardness was lower at higher austenitization temperatures [17].

Choosing the correct austempering temperature is very important because the austempering temperature affects the microstructure (shape and size of the ausferrite) and hardness [1], [10]. At higher austempering temperatures, there is a tendency for strain hardening and increased martensite formation [18], [19]. At lower austempering temperatures, there is a finer austenite size and a greater amount of ferrite, which prevents the formation of martensite caused by strain hardening [18]. The amount of martensite decreased gradually and finally disappeared with increasing austempering time, whereas the transformed austenite content decreased and the amount of acicular ferrite increased [20].

U.R Kumari et al. [19] concluded that at low austempering temperatures (260–300°C), fine bundles of ferrite will form with austenite flakes in between. Such a microstructure results in a high hardness and strength. Meanwhile, at high austempering temperatures (350–400°C), wide ferrite sheaths with blocky austenite are observed. A coarser microstructure, coupled with a large amount of austenite, reduces its strength and hardness. The ausferitic structure gradually decomposed into dispersive cementite particles at higher tempering temperatures.

The aim of this study was to investigate the optimal parameter combinations for ADI. Some parameters that influence ADI include austenitizing temperature, austenitizing time, austempering temperature, and austempering time. In this experiment, parameter combinations of austenitization temperature and austempering time were performed to investigate

the microstructure, hardness, and toughness of ADI. The two other parameters, such as austenitizing time and austempering temperature, were kept constant at 90 min and 350°C, respectively.

2 Research Methods

The nodular cast iron used in this study was supplied as as-cast in Y-block casting, which was made through a melting process in a furnace using several raw materials, including steel scrap, carburizer, and some alloying elements. After that the molten metal is poured into the ladle. Then, the Fe-Si-Mg alloy was added to the ladle to trigger the formation of graphite nodules and Fe-Si-Al-Ca alloy for inoculation. Before the liquid metal was poured into the mold, samples of the liquid metal were collected from inside the ladle to test the chemical composition. This test uses a portable spectrometer to determine the chemical composition of nodular cast iron. After that, the molten metal from the ladle is poured into Y-block shape sand mold (Fig. 1). The results of the chemical composition tests are shown in Table 1.

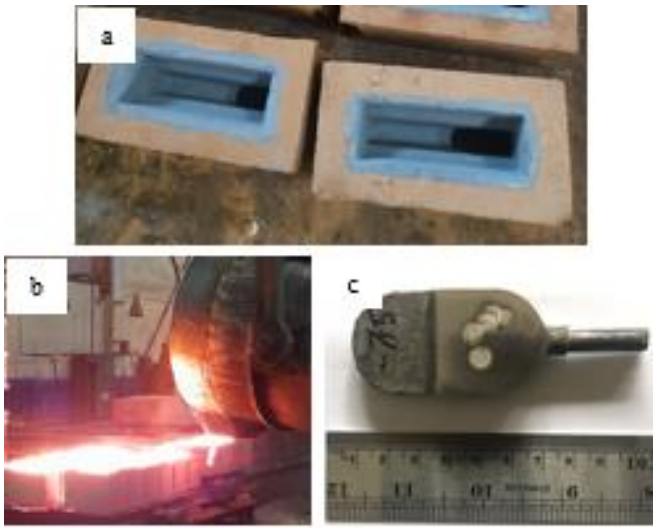

Fig. 1. a) Y-block shape sand mold, b) molten metal poured into Y-block mold, c) specimen for chemical analysis of molten metal.

Table 1. Chemical composition of the experimental nodular cast iron

Chemical composition (wt.%)												
C	Si	Mn	P	S	Cr	Ni	Mo	Mg	Al	Cu	V	Ti
3.45	2.60	0.64	0.030	0.002	0.28	1.58	0.18	0.10	0.026	0.024	0.011	0.013

Fig. 2 shows the nodular cast iron obtained from casting in the Y-block mold used for this experiment. Then the nodular cast iron samples from the Y-block were processed by cutting and machining to produce specimens for hardness tests, impact tests and microstructure observations.

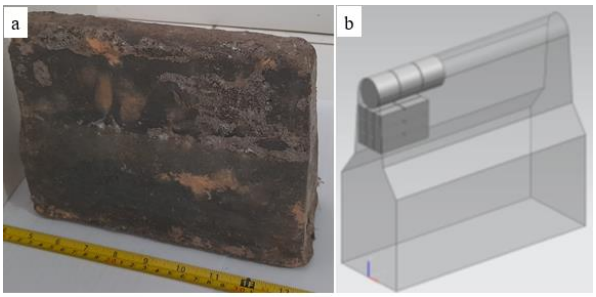

Fig. 2. (a) Y-block casting employed in this study, (b) the location of hardness and impact test specimens in Y- block casting.

The test specimens were then processed by austempering heat treatment to produce ADI. The austempering process was carried out with several variations in austenitizing temperature (850, 900, and 950°C) and austempering time (60, 90, and 120 min). The identity and austempering parameters of each test specimen are shown in Table 2.

Table 2. Parameters used in this study

Sample code	Austeniti-zation temperature (°C)	Austeni-tization time (min)	Austem-pering temperature (°C)	Austem-pering time (min)
ID-1	-	-	-	-
ID-2	850	90	350	90
ID-3	900	90	350	60
ID-4	900	90	350	90
ID-5	900	90	350	120
ID-6	950	90	350	90

The austempering heat treatment cycle is shown in Fig. 3. Initially, the sample was heated in a furnace to the austenitization temperature and held for 90 min to produce a homogeneous austenite phase. The austenitization process used an electric furnace with a maximum heating capacity of 1100°C. Afterwards, austempering was carried out at a temperature of 350°C by immersing it in a salt solution of 50% $NaNO_2$ and 50% $NaNO_3$ and holding it for some time. A muffle furnace was used for the austempering process. After tempering, the test specimens were cooled in the outdoor air until they reached room temperature.

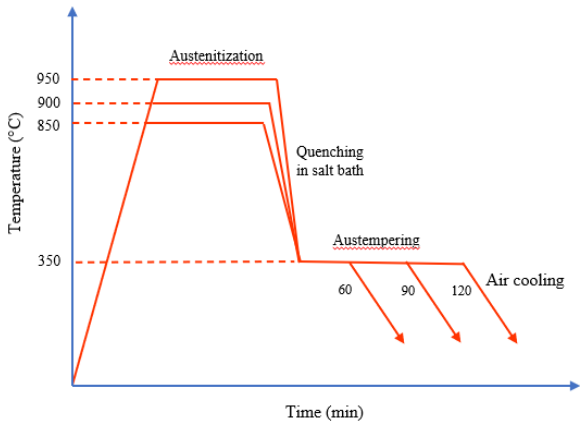

Fig. 3. Austempering heat treatment cycle used in the present study.

Several tests were carried out to analyze the effect of austenitization temperature and tempering time on the microstructure, hardness, and impact toughness. Hardness testing was performed using a Rockwell C hardness tester according to ASTM E18 test standards. This hardness test was carried out at 3 points on each specimen with a dwell time of 10 seconds each. Impact testing was carried out using ASTM E23 standards. There are 3 impact test specimens were used for each parameter, and the final values were the average of three measurements.

Microstructure observation specimens were prepared according to metallographic standards. The metallographic specimens were ground on wet abrasive paper from 60, 120, 240, 400, 600, 800, 1000, and 2000 grit by mechanical instrument, rinsed by water and dried in dry air. Then, it was polished with a cloth and polishing paste to make the surface smoother. Next, etching was carried out using 3% nital etching fluid composed of 3 ml nitric acid (HNO_3) and 97 ml alcohol.

Microstructural observations were carried out using an optical microscope before and after etching. Graphite nodules were treated before etching using an optical microscope at 100× magnification. Observations after etching were performed at 500× magnification to observe the phases formed.

3 Results and Discussion

3.1 Microstructure

Microstructure observations were carried out on as-cast nodular cast iron and nodular cast iron after austempering. The results of observations of the microstructure without etching in as-cast (ID-1) and post-austempered nodular cast iron (ID-2 to ID-6) show the presence of nodular graphite's (see Fig. 4). The graphite shape in all specimens did not show any significant differences. It seems that heat treatment does not change the graphite structure formed in nodular cast iron. Nodular graphite is a stable phase during heat treatment [21].

The observation results of the microstructure after etching show differences between the as-cast and austempered specimens (Fig. 5). Observation results after etching on the as-cast sample (ID-1) show a microstructure consisting of pearlite, ferrite, and graphite. Some carbides were also observed, most likely chromium carbides, due to the high presence of Cr and C elements in the nodular cast iron. The microstructure shows nodular graphite, which looks black, carbide, which looks white, and the combined phase of cementite and ferrite, which forms layers, or what is called pearlite. This carbide structure can increase hardness and cause brittleness. Carbides can dissolve into the austenite phase when held at the austenitization temperature. In the as-cast condition, the ausferrite structure did not appear.

Nodular cast iron that has undergone austempering (ID-2 to ID-6) produces the ausferrite phase. All specimens that underwent austenitization at various austenitization temperatures and tempering times show that there is an ausferrite structure. This structure shows acicular ferrite that looks like long, dark-colored needles. Meanwhile, light-colored retained austenite (carbon-rich austenite) was present between the acicular ferrite.

Samples ID-3 to ID-5 show variations in austempering times of 60, 90, and 120 min, respectively. Meanwhile, the three other parameters (austenitization temperature, austenitization time, and austempering temperature) were kept constant. The microstructure of these samples (Fig. 5) indicates that increasing the austempering time reduced the amount of retained austenite.

3.2 Mechanical Properties

Table 3 shows the results of hardness and impact toughness testing. Test results show that the hardness and impact toughness of the austempered samples (ID-2 to ID-6) increased significantly compared to the as-cast sample (ID-1). Austempering has increased the hardness and impact toughness of nodular cast iron samples. This is due to the changes in the microstructure in the presence of the ausferrite phase.

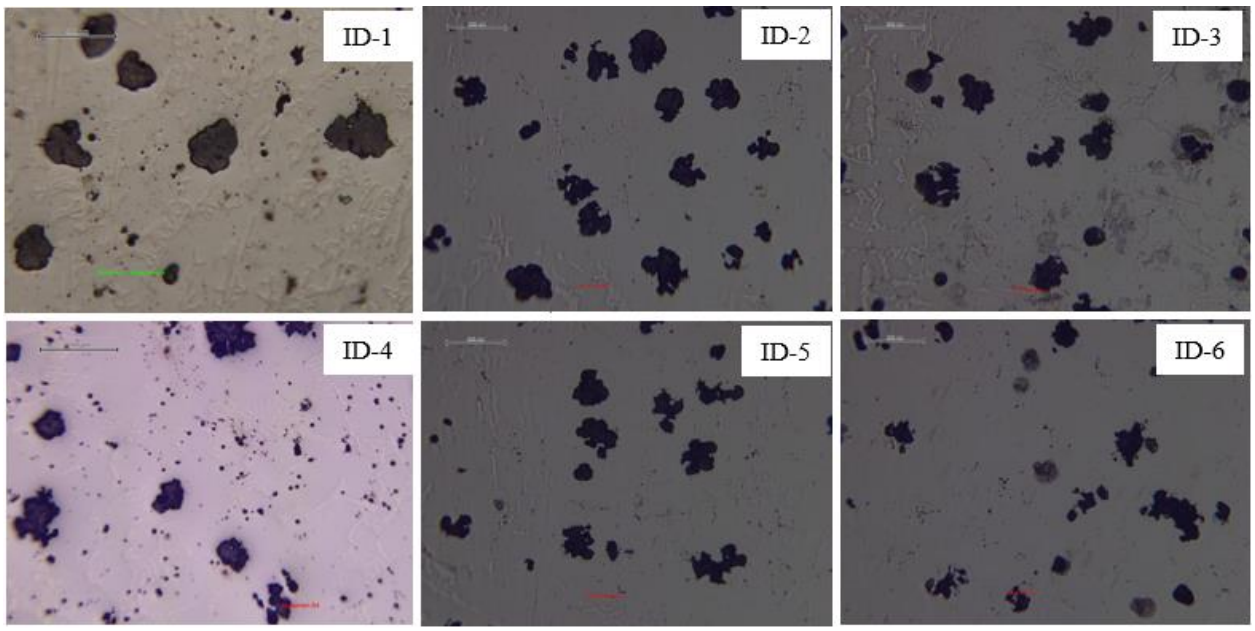

Fig. 4. Microstructure in non-etching conditions (100× magnification).

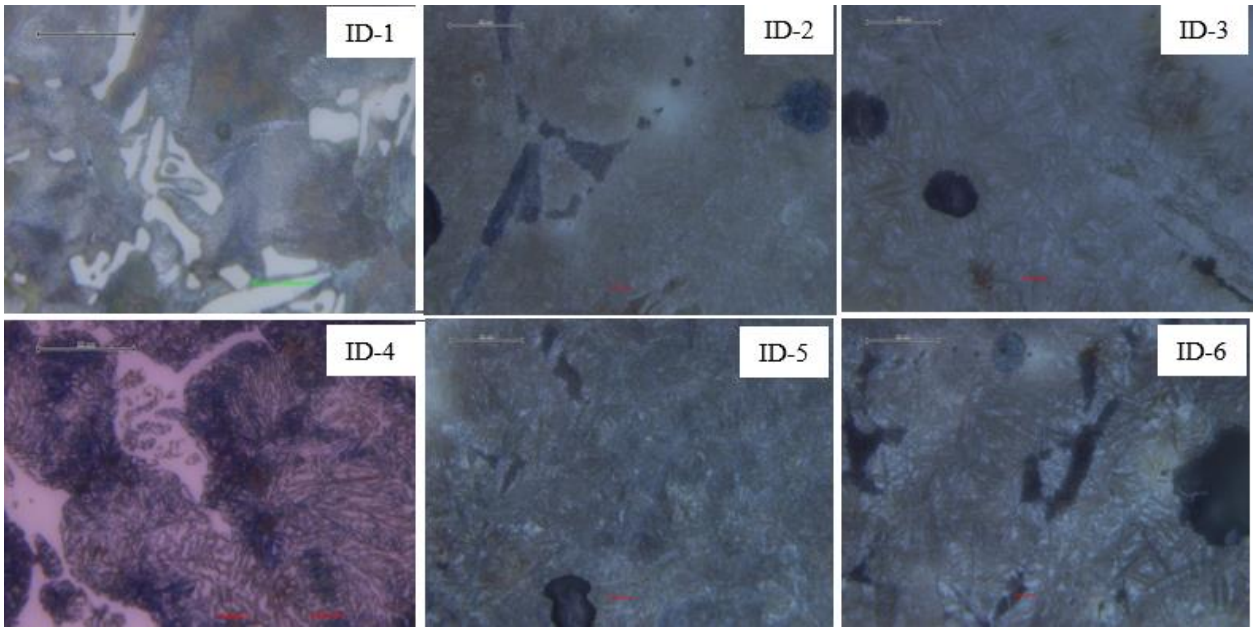

Fig. 5. Microstructure under etching conditions (500× magnification).

Table 3. Hardness and impact test results

Sample ID	Hardness (HRC)	Impact energy (J)
ID-1	41.5	1.9
ID-2	46.8	3.8
ID-3	46.7	2.9
ID-4	44.3	3.9
ID-5	45.1	3.7
ID-6	44.7	3.5

Austempering parameters influence hardness and impact toughness. It was found that differences in austenitization temperature and austempering time affect the hardness and impact toughness values. This can be seen in Fig. 6 and Fig. 7.

Fig. 6 shows the relationship between the austenitization temperature, hardness, and impact toughness. The samples were measured from varying austenitization temperatures of 850˚C (ID-2), 900˚C (ID-4), and 950˚C (ID-6). Each sample was at the same austempering temperature and austempering time (see Table 2).

The measurement results show that samples with an austenitization temperature of 850˚C (ID-2) have higher hardness than austenitization temperatures of 900˚C (ID-4) and 950˚C (ID-6). Meanwhile, the hardness of samples from austenitization results at 900˚C and 950˚C is not much different. Previous research has shown that a higher austenitization temperature can dissolve the carbide, thereby reducing its hardness [17].

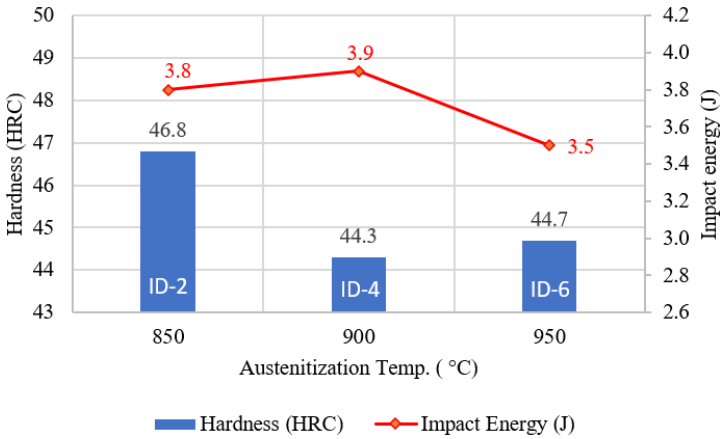

Fig. 6. Effect of austenitization temperature on hardness and impact toughness for samples ID-2, ID-4, and ID-6.

The decrease in hardness affected toughness. The highest impact toughness was seen in samples with an austenitization temperature of 900˚C (ID-4), this result was almost the same as 850˚C (ID-2). Meanwhile, the decrease in hardness in the sample resulting from an austenitization temperature of 950˚C (ID-6) was not accompanied by an increase in toughness. This is likely due to the presence of the martensite phase.

Fig. 7 shows the effect of the austempering time on the hardness and toughness at an austenitization temperature of 950°C and an austempering temperature of 350°C. The differences in the austempering times of 60, 90, and 120 min (ID-3, ID-4, and ID-5, respectively) affect the hardness and toughness values. The hardness value at the austempering time of 60 min (ID-3) was higher than that at 90 min (ID-4), and 120 min (ID-5). Meanwhile, the hardness at austempering times of 90 min (ID-4) and 120 min (ID-5) were not significantly different. The highest impact toughness was observed at an austempering time of 90 min (ID-4) and the lowest was observed at an austempering time of 60 min (ID-3). This was correlated with the increased austempering time, which reduced the retained austenite content.

Based on the test results for all the samples, the highest hardness was obtained for samples ID-2 and ID-3, namely 46.8 and 46.7 HRC, respectively. These are the result of a combination of austenitization temperature and austempering time of 850°C with 90 min, and 900°C with 60 min, respectively. However, if impact toughness is also a concern, then sample ID-2 is worth considering because it has a significantly higher impact energy, namely 3.8 J, compared than ID-3 (2.9 J).

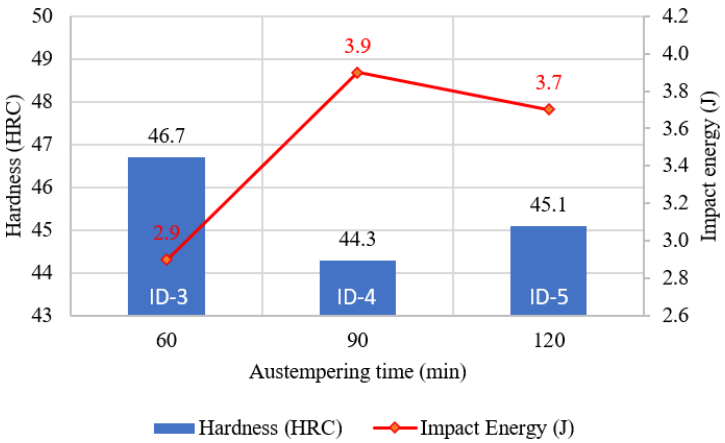

Fig. 7. Effect of austempering time on hardness and impact toughness for samples ID-3, ID-4, and ID-5.

4 Conclusion

The austempering process increased the hardness and toughness of nodular cast iron samples. This is due to the changes in the microstructure, where austempering produces an ausferrite phase. Austempering parameters, such as austenitization temperature and tempering time, influence the hardness and toughness values. Based on the test results, sample ID-2 exhibited the highest hardness (46.8 HRC). This was achieved as a result of the combination of an austenitization temperature of 850°C and an austempering time of 90 min. This sample also had a significantly higher impact energy (3.8 J) than those of the other samples.

References

[1] H. Avdusinovic and A. Gigović-Gekić, “Heat treatment of nodular cast iron,” *Trends Dev. Mach. Assoc. Technol.*, pp. 16–21, 2009.

[2] H. Oktadinata, M. S. Dafi, and D. H. Prajitno, “Microstructure Evolution and Hardness Properties of Nodular Cast Iron for Varying Tempering Time,” *Key Eng. Mater.*, vol. 935, pp. 3–9, 2022.

[3] A. A. Nofal and L. Jekova, “Novel processing techniques and applications of austempered ductile iron,” *J. Univ. Chem. Technol. Metall.*, vol. 44, no. 3, pp. 213–228, 2009.

[4] H. Oktadinata, T. Triantoro, and I. Ardiansyah, “Microstructural Characterization and Mechanical Properties of Austempered Ductile Iron at Different Austempering Temperatures,” in *6th Mechanical Engineering, Science and Technology International conference (MEST 2022)*, 2023, pp. 114–121.

[5] B. Wang, F. Qiu, G. C. Barber, Y. Pan, W. Cui, and R. Wang, “Microstructure, wear behavior and surface hardening of austempered ductile iron,” *J. Mater. Res. Technol.*, vol. 9, no. 5, pp. 9838–9855, 2020.

[6] A. Keleş, R. Cengız, and M. Yildirim, “Effect of Alloying Elements and Technological Parameters of Austempering on the Structure and Mechanical Properties of Ductile Cast Iron (ADI),” *Met. Sci. Heat Treat.*, vol. 65, no. 3, pp. 191–199, 2023.

[7] B. Shakeri, E. Heidari, and S. M. A. Boutorabi, “Effect of isothermal heat treatment time on the microstructure and properties of 4.3% Al austempered ductile iron,” *Int. J. Met.*, vol. 17, no. 4, pp. 3005–3018, 2023.

[8] Z. Shi, M. Dong, Y. Sun, J. Ma, X. Du, and J. Zhao, “Effects of austempering time on the microstructure and properties of austempered ductile iron,” *Metall. Res. Technol.*, vol. 119, no. 1, p. 117, 2022.

[9] A. Uyar, O. Sahin, B. Nalcaci, and V. Kilicli, “Effect of austempering times on the microstructures and mechanical properties of dual-matrix structure austempered ductile iron (DMS-ADI),” *Int. J. Met.*, vol. 16, no. 1, pp. 407–418, 2022.
[10] X. Wang *et al.*, “Relationship among process parameters, microstructure, and mechanical properties of austempered ductile iron (ADI),” *Mater. Sci. Eng. A*, vol. 857, p. 144063, 2022.
[11] S. Singh and B. Singh, “Parametric study and optimization of austenitization and austempering on ductile iron,” in *AIP Conference Proceedings*, 2023, vol. 2800, no. 1.
[12] B. Karaca, M. Şimşir, and H. Akkan, “Effect of heat treatment on the tensile properties of cam shaft made of ductile cast iron,” *J. Achiev. Mater. Manuf. Eng.*, vol. 76, no. 1, pp. 15–20, 2016.
[13] M. Górny, Ł. Gondek, E. Tyrała, G. Angella, and M. Kawalec, “Structure homogeneity and thermal stability of austempered ductile iron,” *Metall. Mater. Trans. A*, vol. 52, pp. 2227–2237, 2021.
[14] L. Maddi, V. Dakre, A. Likhite, and S. Pathak, “Effect of Two-Step Austempering Process on the Microstructure and Mechanical Properties of Low-Carbon Equivalent Austempered Ductile Iron,” *SAE Int. J. Mater. Manuf.*, vol. 17, no. 05-17-01–0004, 2023.
[15] A. S. Darmawan, A. D. Anggono, A. Yulianto, B. W. Febriantoko, and A. Hamid, “Effect of Austempering Holding Time Variations of 30, 60, and 90 Minutes at 300° C on The Microstructure and Toughness of Nodular Cast Iron,” in *Journal of Physics: Conference Series*, 2024, vol. 2739, no. 1, p. 12029.
[16] M. Górny, G. Angella, E. Tyrała, M. Kawalec, S. Paź, and A. Kmita, “Role of austenitization temperature on structure homogeneity and transformation kinetics in austempered ductile iron,” *Met. Mater. Int.*, vol. 25, pp. 956–965, 2019.
[17] V. Dakre, D. R. Peshwe, S. U. Pathak, and A. Likhite, “Effect of austenitization temperature on microstructure and mechanical properties of low-carbon-equivalent carbidic austempered ductile iron,” *Int. J. Miner. Metall. Mater.*, vol. 25, pp. 770–778, 2018.
[18] S. Daber and P. Prasad Rao, “Formation of strain-induced martensite in austempered ductile iron,” *J. Mater. Sci.*, vol. 43, pp. 357–367, 2008.
[19] U. R. Kumari and P. P. Rao, “Study of wear behaviour of austempered ductile iron,” *J. Mater. Sci.*, vol. 44, pp. 1082–1093, 2009.
[20] M. Erdogan, V. Kilicli, and B. Demir, “Transformation characteristics of ductile iron austempered from intercritical austenitizing temperature ranges,” *J. Mater. Sci.*, vol. 44, pp. 1394–1403, 2009.
[21] J. Bai *et al.*, “Microstructures and mechanical properties of ductile cast iron with different crystallizer inner diameters,” *Crystals*, vol. 12, no. 3, p. 413, 2022.